

Sensorless Control of IPMSM for Last 10 Years and Next 5 Years

Seung-Ki Sul, *Fellow, IEEE*, Yong-Cheol Kwon, and Younggi Lee

(Invited)

Abstract—This paper presents the developments of sensorless control of interior permanent magnet synchronous machine (IPMSM) for last 10 years, which could be divided into the past and the present for each 5 years. Several popular methods developed for last 10 years would be described and evaluated, and the limitations with the methods are discussed. In the past a concept extended EMF (EEMF) was introduced and it can model IPMSM as a non-salient motor, meaning that the representation of IPMSM in the estimated rotor reference frame would be much simpler and accurate. However, because it still relied on back EMF, standstill operation was impossible. And, the position control of IPMSM could not be achieved with EEMF concept. For sensorless drive, the high-frequency signal injection method exploiting inherent saliency of IPMSM has been continuously developed for last 10 years and applied to various industry fields, where torque control at standstill is essential. Its performance has been improved but there are still many problems to be solved. In the present, the square-wave signal injection at estimated d-axis has improved the control performance conspicuously. However, there are strong demands to improve the control performance of sensorless drive, yet. Based on the problems in the present, in this paper the possible developments of sensorless drive of IPMSM in next 5 years are enlightened as the future of sensorless control.

Index Terms—Back EMF, extended EMF method, high-frequency signal injection method, interior permanent magnet synchronous motor, review, sensorless control.

I. INTRODUCTION

SENSORLESS drive of interior permanent magnet synchronous machine (IPMSM) has been evolved in the beginning of the introduction of IPMSM itself. The existing methods developed for sensorless control of induction machine had been modified and applied to IPMSM [1-3]. Because those methods were based on back EMF of the machine, its operating range had been inherently limited. But around 20 years ago, a sensorless control method based on high-frequency (HF) sinusoidal signal injection had opened new horizon of sensorless control of IPMSM [4-9]. Thanks to the method, with the most of IPMSM the zero frequency operation at full torque in transient and steady state had been possible. It had been commercialized and proved its effectiveness in many industrial

fields. The methods based on back EMF had been evolved too and a method based on extended EMF in conjunction with observers revealed reasonable performance down to a few percent of the rated speed and it also had been used in many industrial fields [10-15]. But the accuracy, speed control bandwidth, and operating speed of sensorless drive had been far limited compared to those of sensed drive with a couple hundred pulses per revolution (PPR) encoder. For the last 5 years, which is the present time in this paper, based on the square-wave signal injection the bandwidths of speed and position control have been enhanced by at least 5 times and the bandwidths are comparable to sensed drive with low resolution encoder [16-19]. Not only electrical angle of the rotor, but also the absolute angle of IPMSM has been estimated with slightly modified design of IPMSM. And, control of the absolute rotor position in the sense of the mechanical angle had been possible [20-22].

But still there are problems and areas for the developments. If IPMSM is highly saturated, the saliency disappears and is even reversed. And, sensorless control based on the signal injection would not be possible in this region [23, 24]. For identification of the absolute angle in sensorless control, the initial motion is inevitable or there should be extra coils and connections for no initial motion, and those are not desirable [20-22]. Also, sensorless drive for linear PMSM has not been fully investigated yet. Because of the end effect due to its limited mover size sensorless control of linear PMSM would be still an open question [25-27].

II. PAST

Sensorless control methods based on mathematical model have been proposed since early 1990s. In the beginning, isotropic motors, that is, motors without the inductance saliency, were mainly focused on. They can be represented as follows in the rotor reference frame.

$$\begin{bmatrix} v_{ds}^r \\ v_{qs}^r \end{bmatrix} = \begin{bmatrix} R_s & -\omega_r L_s \\ \omega_r L_s & R_s \end{bmatrix} \begin{bmatrix} i_{ds}^r \\ i_{qs}^r \end{bmatrix} + L_s \frac{d}{dt} \begin{bmatrix} i_{ds}^r \\ i_{qs}^r \end{bmatrix} + \begin{bmatrix} 0 \\ \omega_r \lambda_f \end{bmatrix} \quad (1)$$

In (1), superscript ‘r’ indicates the rotor reference frame. In sensorless drive, however, since it is impossible to accurately estimate the position all the time, the mathematical model in (1) is generally represented and analyzed in the estimated rotor reference frame by

Seung-Ki Sul is with Electrical and Computer Engineering Department, Seoul National University (e-mail: sulsk@plaza.snu.ac.kr).

Yong-Cheol Kwon is with Electrical and Computer Engineering Department, Seoul National University.

Younggi Lee is with Electrical and Computer Engineering Department, Seoul National University.

$$\begin{bmatrix} v_{ds}^r \\ v_{qs}^r \end{bmatrix} = \begin{bmatrix} R_s & -\omega_r L_{qs} \\ \omega_r L_{ds} & R_s \end{bmatrix} \begin{bmatrix} i_{ds}^r \\ i_{qs}^r \end{bmatrix} + L_{qs} \frac{d}{dt} \begin{bmatrix} i_{ds}^r \\ i_{qs}^r \end{bmatrix} + \omega_r \lambda_f \begin{bmatrix} -\sin \tilde{\theta}_r \\ \cos \tilde{\theta}_r \end{bmatrix}. \quad (2)$$

In (2), superscript 'r' means the estimated rotor reference frame. As seen in (2), the back EMF terms include the position estimation error, $\tilde{\theta}_r$, defined as difference between the real and estimated positions, i.e., θ_r and $\tilde{\theta}_r$, respectively. Using this principle, a sensorless control method [1] was proposed where θ_r was estimated by suppressing the difference between (1) and (2). Since this method has shown reasonable control performance for decades, it is still widely accepted in the industrial fields. However, it encounters some problems when applied to the salient motors modeled as (3).

$$\begin{bmatrix} v_{ds}^r \\ v_{qs}^r \end{bmatrix} = \begin{bmatrix} R_s & -\omega_r L_{qs} \\ \omega_r L_{ds} & R_s \end{bmatrix} \begin{bmatrix} i_{ds}^r \\ i_{qs}^r \end{bmatrix} + \begin{bmatrix} L_{ds} & 0 \\ 0 & L_{qs} \end{bmatrix} \frac{d}{dt} \begin{bmatrix} i_{ds}^r \\ i_{qs}^r \end{bmatrix} + \begin{bmatrix} 0 \\ \omega_r \lambda_f \end{bmatrix}. \quad (3)$$

This is because the transformation of (3) into the estimated rotor reference frame results in (4) which contains much complicated inductance matrices and the difference between (3) and (4) does not provide simple information to process any more.

$$\begin{bmatrix} v_{ds}^r \\ v_{qs}^r \end{bmatrix} = R_s \begin{bmatrix} i_{ds}^r \\ i_{qs}^r \end{bmatrix} + \begin{bmatrix} \Sigma L_s + \Delta L_s \cos 2\tilde{\theta}_r & \Delta L_s \sin 2\tilde{\theta}_r \\ \Delta L_s \sin 2\tilde{\theta}_r & \Sigma L_s - \Delta L_s \cos 2\tilde{\theta}_r \end{bmatrix} \frac{d}{dt} \begin{bmatrix} i_{ds}^r \\ i_{qs}^r \end{bmatrix} + \omega_r \begin{bmatrix} -\Delta L_s \sin 2\tilde{\theta}_r & -\Sigma L_s + \Delta L_s \cos 2\tilde{\theta}_r \\ \Sigma L_s + \Delta L_s \cos 2\tilde{\theta}_r & \Delta L_s \sin 2\tilde{\theta}_r \end{bmatrix} \begin{bmatrix} i_{ds}^r \\ i_{qs}^r \end{bmatrix} + \omega_r \lambda_f \begin{bmatrix} -\sin \tilde{\theta}_r \\ \cos \tilde{\theta}_r \end{bmatrix}. \quad (4)$$

In [2]-[3], a concept of extended EMF (EEMF) defined as (5) was introduced.

$$E_{ex} \equiv \omega_r \lambda_f + 2\omega_r \Delta L_s i_{ds}^r - 2\Delta L_s p i_{qs}^r. \quad (5)$$

By using the definition of EEMF, the voltage equation in (3) can be simplified as follows.

$$\begin{bmatrix} v_{ds}^r \\ v_{qs}^r \end{bmatrix} = \begin{bmatrix} R_s & -\omega_r L_{qs} \\ \omega_r L_{ds} & R_s \end{bmatrix} \begin{bmatrix} i_{ds}^r \\ i_{qs}^r \end{bmatrix} + L_{ds} \frac{d}{dt} \begin{bmatrix} i_{ds}^r \\ i_{qs}^r \end{bmatrix} + \begin{bmatrix} 0 \\ E_{ex} \end{bmatrix}. \quad (6)$$

The voltage equation in the estimated rotor reference frame can be expressed as

$$\begin{bmatrix} v_{ds}^f \\ v_{qs}^f \end{bmatrix} = \begin{bmatrix} R_s + pL_{ds} & -\omega_r L_{qs} \\ \omega_r L_{qs} & R_s + pL_{ds} \end{bmatrix} \begin{bmatrix} i_{ds}^f \\ i_{qs}^f \end{bmatrix} + \begin{bmatrix} e_{ds}^f \\ e_{qs}^f \end{bmatrix}, \quad (7)$$

$$\text{where } \begin{bmatrix} e_{ds}^f \\ e_{qs}^f \end{bmatrix} = E_{ex} \begin{bmatrix} -\sin \tilde{\theta}_r \\ \cos \tilde{\theta}_r \end{bmatrix} + \tilde{\omega}_r L_{ds} \begin{bmatrix} i_{qs}^f \\ -i_{ds}^f \end{bmatrix}.$$

Note that inductance matrices become symmetric in (6), making a salient motor such as IPMSM be seen as a non-salient motor. Thanks to this feature, the representation in (7) is much simpler than that in (4). Using the EEMF estimator in Fig. 1, the EMF terms, e_{dqs}^f , can be obtained. Then, $\tilde{\theta}_r$ can be easily estimated by arctangent or simple arithmetic calculation of e_{dqs}^f [2].

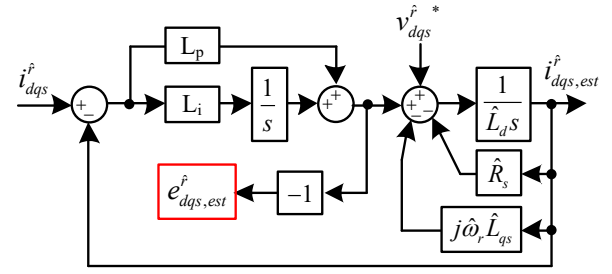


Fig. 1. EEMF estimator for IPMSM.

From the estimated value of $\tilde{\theta}_r$, $\tilde{\theta}_{r,est}$, the estimation of the rotor position without phase lagging is also necessary [10]. Fig. 2 shows a position and speed estimator using $\tilde{\theta}_{r,est}$ as an input. In this position estimator, zero phase lag could be achieved under the assumption of accurate mechanical parameters by feed-forwarding the torque into the estimator. Enhanced estimation performance of the estimator in Fig. 2 was verified by experiments where the position estimation error had a little transient less than a few degrees even to the rated step load change at 2,700 r/min [10].

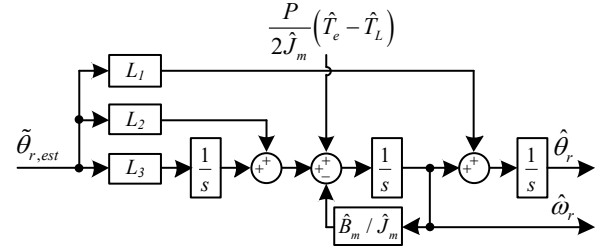


Fig. 2. Position and speed estimator including feedforward input.

The effects of inaccurate parameters on model-based sensorless drive has been analyzed [28-30]. From the analysis, it has been revealed that parameter errors on the resistance and q-axis inductance (i.e., R_s and L_{qs}) have critical effects on the performance; Generally, R_s is very influential at low speed where the resistive voltage drop is relatively large compared to the EMF voltage. While, the effect of L_{qs} is independent of the rotational speed, ω_r . For this reason, parameter identification is essential, especially for R_s and L_{qs} . However, since many algorithms have been derived under the assumption that the position estimation error is negligible, it may lead to incorrect parameter estimation and deteriorates the performance [11, 12].

Against the parameter variation, rather than parameter identification, robust estimators such as an adaptive observer can be used [13, 14]. In an adaptive observer, gains should be set considering the stability at each operating point, robustness, and response. Even if it could cause instability with the improper gains or the parameter error over the allowable range, robust estimators against the parameter variation could be designed.

Typically, model-based methods show a satisfactory performance above 10% of the rated speed. At lower speed, estimated back EMF decreases and the effects of harmonics and

noise components increases. Therefore, at lower speed, the bandwidth of the position estimator also should be reduced to filter o harmonic frequency and trace the fundamental component [15]. However, it is hard to expect reasonable performance in most industrial drives at lower than a few percent of the rated speed.

Meanwhile, Boldea *et al.* [31] introduced a concept of active flux, Ψ_a , which is defined as follows.

$$\Psi_a \equiv \lambda_f + (L_{ds} - L_{qs}) i_{ds}^r \quad (8)$$

Using active flux, the flux equation can be simplified as (9).

$$\begin{bmatrix} \lambda_{ds}^r \\ \lambda_{qs}^r \end{bmatrix} = L_{qs} \begin{bmatrix} i_{ds}^r \\ i_{qs}^r \end{bmatrix} + \begin{bmatrix} \Psi_a \\ 0 \end{bmatrix} \quad (9)$$

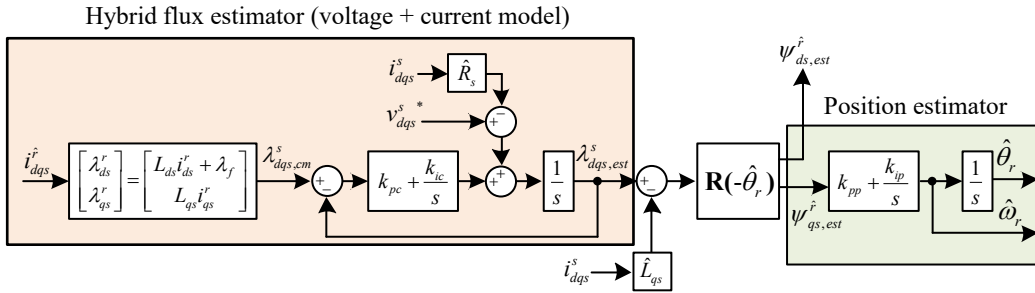


Fig. 3. Active flux estimator and position/speed estimator [31].

Another main category for sensorless control is based on magnetic saliency of the motor. Since spatial inductance distribution mainly has 2nd harmonic in one electrical period as shown in Fig. 4, many position estimation algorithms using the inductance characteristics have been proposed [4-9], [32-35]. In saliency tracking methods, since the speed-dependent information such as back EMF is not required, operating region of sensorless drive can be extended to very low speed including standstill.

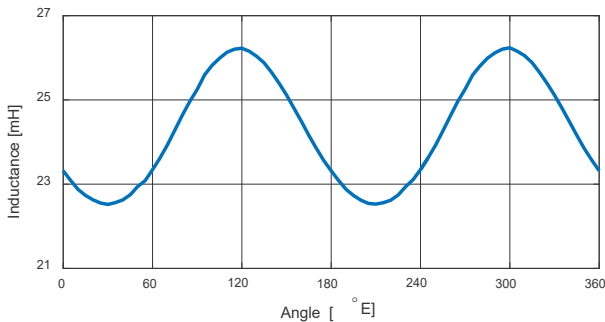


Fig. 4. Spatial inductance distribution of IPMSM at $\theta_r = 30^\circ$.

In its embryonic stage, current ripple was utilized to calculate inductances during one PWM period [32-34], or discrete test voltage was injected to obtain the position information [35]. However, these methods required the variable switching period or the manipulation of PWM methods. Then, continuous sinusoidal injection methods were addressed without any variation of PWM methods or switching frequency [4-9]. Continuous injection methods are generally classified

Similar to EEMF does, active flux makes a salient motor such as IPMSM be seen as a non-salient motor. This simplifies the flux equation in the estimated rotor reference frame as (10).

$$\begin{bmatrix} \lambda_{ds}^r \\ \lambda_{qs}^r \end{bmatrix} = L_{qs} \begin{bmatrix} i_{ds}^r \\ i_{qs}^r \end{bmatrix} + \begin{bmatrix} \psi_{ds}^r \\ \psi_{qs}^r \end{bmatrix} \quad (10)$$

where $\begin{bmatrix} \psi_{ds}^r \\ \psi_{qs}^r \end{bmatrix} = \begin{bmatrix} \Psi_a \cos \tilde{\theta}_r \\ \Psi_a \sin \tilde{\theta}_r \end{bmatrix}$

Since the projected active flux on q-axis ψ_{qs}^r , is almost proportional to the position error, the position and speed can be estimated by nullifying ψ_{qs}^r as shown in Fig. 3.

into two categories depending on where and how the signal is injected: rotating voltage signal injection in the stationary reference frame [4-6] and pulsating voltage signal injection in the estimated rotor reference frame [7-9]. These sensorless control methods have their unique characteristics according to the injection signal.

Firstly, in rotating signal injection case, injected rotating signal is expressed as (11) and current response can be derived as (12).

$$\begin{bmatrix} v_{dsh}^{s*} \\ v_{qsh}^{s*} \end{bmatrix} = V_h \begin{bmatrix} -\sin \omega_h t \\ \cos \omega_h t \end{bmatrix} \quad (11)$$

$$\begin{bmatrix} i_{dsh}^s \\ i_{qsh}^s \end{bmatrix} = \frac{V_h}{\omega_h} \frac{\Sigma L_{sh}}{\Sigma L_{sh}^2 - \Delta L_{sh}^2} \begin{bmatrix} \cos \omega_h t \\ \sin \omega_h t \end{bmatrix} - \frac{V_h}{\omega_h} \frac{\Delta L_{sh}}{\Sigma L_{sh}^2 - \Delta L_{sh}^2} \begin{bmatrix} \cos(2\theta_r - \omega_h t) \\ \sin(2\theta_r - \omega_h t) \end{bmatrix} \quad (12)$$

In HF range where the additional signal is injected, the injection frequency, ω_h , is much larger than ω_r and resistive drop in (3) can be neglected. Therefore, in (12), the motor is modeled as an inductive load. From (12), $\tilde{\theta}_{r,est}$ can be obtained through a demodulation process such as (13).

$$\tilde{\theta}_{r,est} = \frac{\omega_h (\Sigma L_{sh}^2 - \Delta L_{sh}^2)}{2 \Delta L_{sh} V_h} \times \text{LPF} \left\{ -i_{dsh}^s \sin(2\hat{\theta}_r - \omega_h t) + i_{qsh}^s \cos(2\hat{\theta}_r - \omega_h t) \right\} \quad (13)$$

Then, the estimated error in (13) is used as an input to the estimator in Fig. 2 and the position and speed can be estimated

in the direction that the error in (13) is nullified.

Meanwhile, there is another approach to the saliency tracking based on the injection of pulsating signal at the estimated d-axis as expressed in (14).

$$\begin{bmatrix} v_{dsh}^{\hat{r}} \\ v_{qsh}^{\hat{r}} \end{bmatrix} = V_h \begin{bmatrix} \cos \omega_h t \\ 0 \end{bmatrix} \quad (14)$$

Similar with the rotating signal case in (12), HF current response and $\tilde{\theta}_{r,est}$ can be expressed as (15) and (16), respectively.

$$\begin{bmatrix} i_{dsh}^{\hat{r}} \\ i_{qsh}^{\hat{r}} \end{bmatrix} = \frac{V_h}{\omega_h (\Sigma L_{sh}^2 - \Delta L_{sh}^2)} \begin{bmatrix} (\Sigma L_{sh} - \Delta L_{sh} \cos 2\tilde{\theta}_r) \sin \omega_h t \\ -\Delta L_{sh} \sin 2\tilde{\theta}_r \sin \omega_h t \end{bmatrix} \quad (15)$$

$$\tilde{\theta}_{r,est} = \frac{-\omega_h (\Sigma L_{sh}^2 - \Delta L_{sh}^2)}{\Delta L_{sh} V_h} \times \text{LPF} \left(i_{qsh}^{\hat{r}} \sin \omega_h t \right) \quad (16)$$

In HF signal injection sensorless methods including rotating and pulsating signal injection, two methods seem to be similar with each other. However, many comparison results were presented [36-40]. From various researches, it has been

$$\frac{d}{dt} \begin{bmatrix} i_{dsh}^{\hat{r}} \\ i_{qsh}^{\hat{r}} \end{bmatrix} = \frac{1}{\Sigma L_{sh}^2 - \Delta L_{sh}^2 - L_{dqsh}^2} \begin{bmatrix} \Sigma L_{sh} - \Delta L_{sh} \cos 2\tilde{\theta}_r + L_{dqsh} \sin 2\tilde{\theta}_r & -\Delta L_{sh} \sin 2\tilde{\theta}_r - L_{dqsh} \cos 2\tilde{\theta}_r \\ -\Delta L_{sh} \sin 2\tilde{\theta}_r - L_{dqsh} \cos 2\tilde{\theta}_r & \Sigma L_{sh} + \Delta L_{sh} \cos 2\tilde{\theta}_r - L_{dqsh} \sin 2\tilde{\theta}_r \end{bmatrix} \begin{bmatrix} v_{dsh}^{\hat{r}} \\ v_{qsh}^{\hat{r}} \end{bmatrix} \quad (18)$$

From (18), the resulting estimation error in steady state can be deduced as (19) by replacing the q-axis current variation with zero [41].

$$\tilde{\theta}_r = -\frac{1}{2} \tan^{-1} \left(\frac{L_{dqsh}}{\Delta L_{sh}} \right) \quad (19)$$

On top of the cross-coupling inductance, inherent spatial inductance harmonics and reduced saliency by saturation should be considered for high performance sensorless drive [23], [42]. Basically, in IPMSM case, each phase inductance mainly consists of DC and multiples of 2nd harmonic components which appear as multiples of 6th harmonic components in the rotor reference frame. Since these components result in the position estimation error mainly with 6th harmonic from (19), operating performance could be enhanced by decoupling these major harmonic components according to the operating conditions and tracking the fundamental component [42]. In addition, the saliency is getting smaller as the load increases due to the magnetic saturation. And, the feasible operating region needs to be investigated considering the reduced saliency. Ref. [23] analyzed the feasibility region of signal injection sensorless control for IPMSM in machine-design point of view.

III. PRESENT

In both model-based and HF signal injection methods, improvement of the position estimation accuracy and dynamic

revealed that pulsating signal injection is more robust to different geometry per pole, i.e., mechanical asymmetry among electrical periods [36] and dead time [37, 38]. Also, naturally, pulsating signal injection methods generate less torque ripple [39] and less additional loss under the same magnitude of $\tilde{\theta}_{r,est}$.

In addition, in HF signal injection sensorless drive, the importance of the cross-coupling effects has been emphasized for better performance [23], [41, 42]. Considering the cross-coupling effect, off-diagonal elements in the inductance matrix should be taken into account. Then, HF equivalent voltage equation can be expressed as (17).

$$\begin{bmatrix} v_{dsh}^r \\ v_{qsh}^r \end{bmatrix} = \begin{bmatrix} L_{dsh} & L_{dqsh} \\ L_{qdsh} & L_{qsh} \end{bmatrix} \frac{d}{dt} \begin{bmatrix} i_{dsh}^r \\ i_{qsh}^r \end{bmatrix} \quad (17)$$

Transforming (17) into the estimated rotor reference frame, HF current variation induced by the voltage injection can be derived as (18).

performance has been an important issue since sensorless drive has begun to be considered in the servo application. For better position estimation accuracy, various research has been conducted: more precise modeling of IPMSM considering the cross-coupling inductance, compensation of voltage disturbance by the inverter nonlinearity, identification of system parameters, etc., as aforementioned in the previous chapter.

Regarding the dynamic performance, some of the recent studies have contributed to the enhanced control performance. In HF sinusoidal signal injection methods, generally, the injection frequency should be set between the current control bandwidth and the PWM switching frequency. Using a general purpose IGBT inverter with 10 kHz switching frequency, the injection frequency had been set as 500 Hz~700 Hz, which confined the current control bandwidth under 100 Hz~200 Hz. Sequentially, it had been difficult to increase bandwidths of speed and position controllers.

This limitation can be overcome by increasing the injection frequency, making it possible to increase bandwidths of current, speed, and position controllers. In order to do this, Yoon *et al.* [16] proposed square-wave signal injection method increasing the injection frequency to a half of the PWM switching frequency. Fig. 5 shows typical voltage and current waveforms under square-wave signal injection. Eq. (20) represents the injection voltage reference in a discretized form according to the sampling count n [17, 18].

$$\begin{bmatrix} v_{dsh}^r \\ v_{qsh}^r \end{bmatrix} = \begin{bmatrix} v_{inj}^*[n] \\ 0 \end{bmatrix} \text{ where } v_{inj}^*[n] = \begin{cases} V_h & (n = 4m, 4m+1) \\ -V_h & (n = 4m+2, 4m+3) \end{cases} \quad (20)$$

and m is an integer

HF current variation induced by the injection voltage (20) can be expressed as

$$\begin{bmatrix} \Delta i_{ds}^r \\ \Delta i_{qs}^r \end{bmatrix} = \frac{T_s}{L_{dsh} L_{qsh}} \begin{bmatrix} \Sigma L_{sh} - \Delta L_{sh} \cos 2\tilde{\theta}_r \\ -\Delta L_{sh} \sin 2\tilde{\theta}_r \end{bmatrix} \cdot v_{inj}^*[n-2] \quad (21)$$

From the q-axis current variation in (21), $\tilde{\theta}_{r,est}$ can be directly obtained as follows.

$$\tilde{\theta}_{r,est}[n] = \Delta i_{qsh}^r[n] \cdot \left(-\frac{L_{dsh} L_{qsh}}{2T_s \cdot \Delta L_{sh}} \right) \frac{1}{v_{inj}^*[n-2]} \approx \tilde{\theta}_r \quad (22)$$

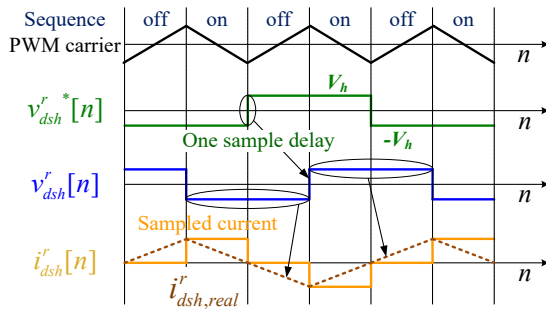


Fig. 5. HF signal injection voltage and HF current in square-wave signal injection sensorless drive.

Using the square-wave signal injection, $\hat{\theta}_{r,est}$ can be obtained with a delay of two sampling periods, which makes it possible to increase overall control bandwidths. Ref. [16] reported that the bandwidths of speed and position controllers could extend up to 40 Hz and 10 Hz, respectively, with an 80-Watt general-purpose IPMSM. Fig. 6 shows speed and position responses to sinusoidal 50 Hz speed and 10 Hz position references, respectively.

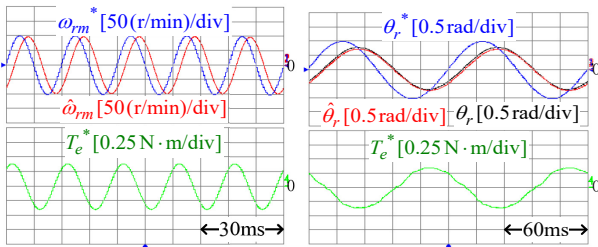


Fig. 6. Speed and position control performance with square-wave signal injection [16].

In [19], Kim *et al.* increased the injection frequency up to the PWM switching frequency. This makes it possible to increase the injection frequency almost above the range of human hearing in the case of over 16 kHz switching frequency. Thus, the audible noise by the signal injection can be virtually eliminated. Under switching-frequency signal injection, the injection frequency is a half of the sampling frequency. Fig. 7 shows current and voltage waveforms under switching-frequency signal injection. Separation of

fundamental and HF currents is difficult since it is impossible to implement the notch filter due to the Nyquist theorem. Considering current variations by both fundamental and HF signal injection voltages, Kim *et al.* [19] had proposed a simple demodulation method utilizing recent three samples of the current to separate fundamental and HF components as shown in Fig. 7.

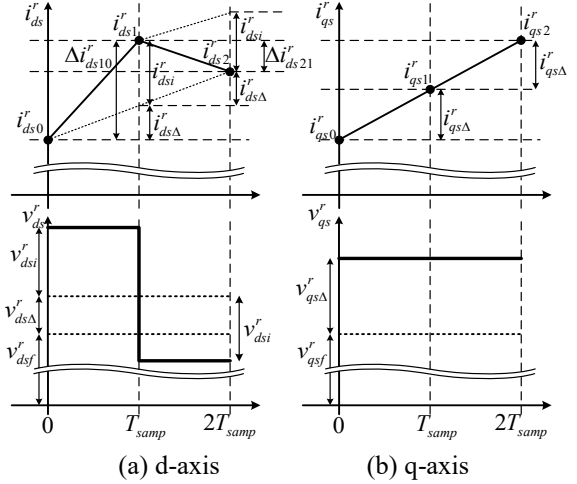


Fig. 7. dq-axes currents and voltages under PWM switching frequency signal injection [19].

In signal injection sensorless drives, the signal injection causes undesirable effects such as acoustic noise, reduced voltage margin of the inverter, and HF losses. These problems can be relieved by reducing the magnitude of the injection voltage, V_h . However, V_h cannot be lower than a certain value due to the inverter nonlinearity. In [18], Kim *et al.* proposed HF current ripple regulator shown in Fig. 8 to attenuate voltage disturbance by the inverter nonlinearity. In conventional signal injection sensorless methods using fixed V_h , HF current ripple signal can be severely distorted due to the inverter nonlinearity. In [18], V_h is adjusted to regulate HF current ripple. This makes the voltage disturbance more evenly distributed, reducing rms value of the voltage disturbance. The proposed method conspicuously reduces the position estimation error without increasing the current ripple.

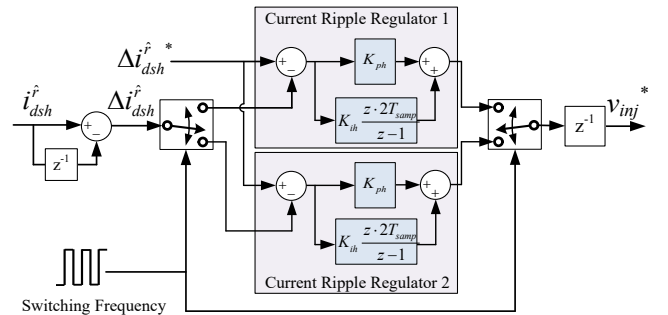


Fig. 7. Block diagram of proposed HF current ripple regulator [18].

Most research conducted into sensorless control so far has focused on the estimation of the rotor position in electrical angle, θ_r since it has been enough for most applications only requiring the torque/speed control. However, the absolute rotor position, θ_{rm} , should be identified and controlled in some

applications such as control of robot arms and machine tools. In usual AC motors, their inductances are repeated per every electrical revolution ($\theta_r = 2\pi$), which makes it difficult to identify θ_{rm} . Thus, modification of the motor design is essential for the absolute rotor position estimation.

In [20-22], Kwon *et al.* proposed possible solutions for absolute position sensorless drive. In [21], two asymmetric IPMSMs named as hole-type and shaving-type motors were proposed for absolute position sensorless drive. Fig. 9 shows the structure of the hole-type motor. At the stator, coils with non-uniform turns ($N_2 > N_1$) are wound. The rotor has two characteristic regions denoted as CR1 and CR2 where small holes are dug. Due to the asymmetry at both stator and rotor, synchronous inductances, L_{ds} and L_{qs} , vary according to θ_{rm} . Utilizing this feature, the absolute rotor position can be estimated from the information of HF current ripple induced by HF voltage injection. However, the rotor has to be aligned to distinct positions to obtain HF current ripple information. This brings about undesirable initial motion of the rotor which is $30^\circ M$ in the worst case.

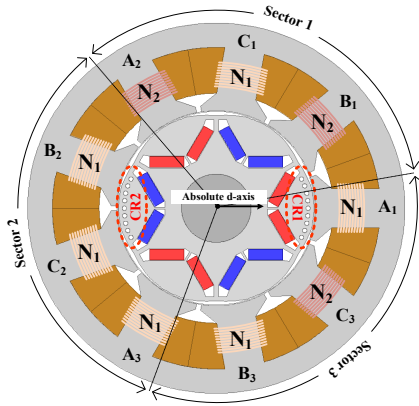
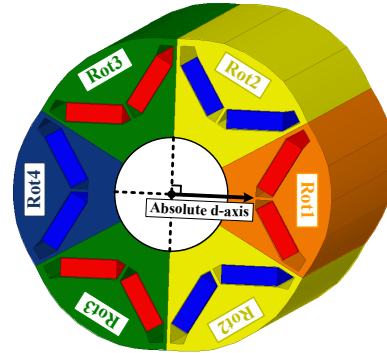


Fig. 8. Hole-type motor for absolute position sensorless drive [21].

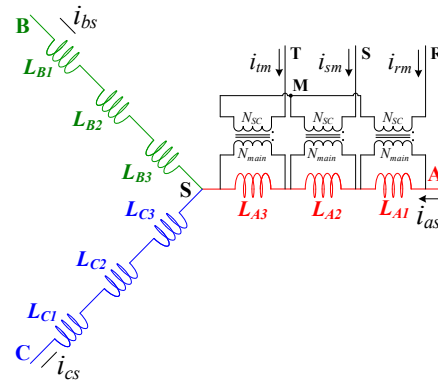
In [22], an IPMSM design named as search-coiled motor for absolute position sensorless drive without the initial motion had been proposed. Fig. 9 shows the structure of the search-coiled motor. At the stator, the search coils are wound at a-phase teeth. The search coils work as voltage transformers converting the input voltage applied to the main winding to another three-phase voltage. In order to measure the voltage signal, two analog-to-digital converter (ADC) channels are required. The rotor consists of differently shaved rotor pieces. The airgap length along the rotor circumference can be modulated by the shaving the surface of the rotor. In the proposed motor, the rotor dimension is optimized to selectively increase 1st order inductance according to θ_{rm} , i.e., $L_1 \cos(\theta_{rm} + \phi)$. This 1st order inductance can be reflected in the voltage signal at the search coils. Using the search-coiled motor, the absolute rotor position can be estimated without any initial motion of the rotor.

Meanwhile, in model-based sensorless drive, there was recent study to enhance the robustness to the load disturbance during sensorless operation. In [43], Lee and *et al.* proposed a model-based sensorless method utilizing the speed error information as well as the position error information. Using this

method, abrupt load disturbances to the sensorless drive system can be effectively handled. Based on the extraction of the position and speed errors in manipulated voltage equation, the position and speed are estimated in separated estimators as shown in Fig. 11. The auxiliary speed estimator in Fig. 11 enhances the speed estimation without increasing the noise sensitivity of the estimated position in the main estimator. Fig. 12 shows the improved dynamic performance of the method. In the figure, the conventional method means that there is no additional speed estimator and input to the observer is $\hat{\theta}_{r,est}$ only. While, in the proposed 1 method both speed and position errors are used as inputs to the observers without auxiliary speed estimator. The proposed 2 method means that there is an auxiliary speed estimator and its output is used as input to the observer. Fig. 12(a) shows the estimation capability during the abrupt speed variation (20,000 r/min/s) in current control mode and Fig. 12(b) shows the speed control performance against the load torque variation at 500 r/min with three different methods. It shows that the method with the auxiliary estimator (proposed 2) reveals much faster response and the robustness to abrupt load variation as well as speed variation.

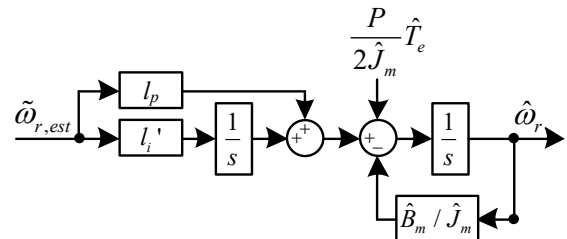


(a) Rotor structure.

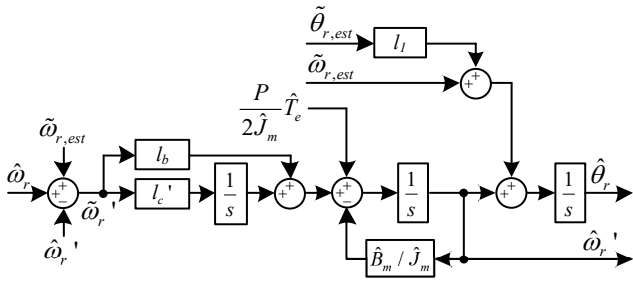


(b) Winding configuration

Fig. 9. Search-coiled motor for absolute position sensorless drive [22].

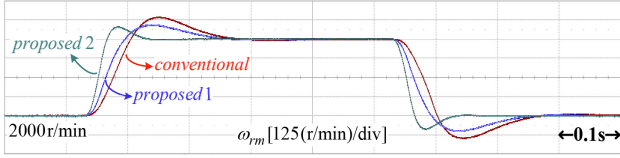


(a) Auxiliary speed estimator.

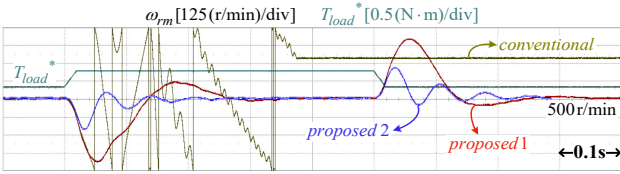


(b) Position estimator.

Fig. 10. Position and speed estimator including the auxiliary speed estimator [43].



(a) Abrupt speed variation (20,000 r/min/s) in current control mode.



(b) Abrupt load torque disturbance (20 p.u./s) in speed control mode.

Fig. 11. Experimental verification for increased robustness [43].

IV. FUTURE

For last 20 years the technology for sensorless drive of IPMSM has been evolved and it has been matured. But still, there are many unsolved issues and problems. At first, sensorless control of linear motor has not been much investigated. The initial position of the mover of the linear motor is essential in the torque control of the motor and it is critically important especially in vertical motion. Contrary to the rotary motor, where slot and coil are continued infinitely, linear motor has end slots and end coils at left and right ends of the mover as shown in Fig. 13. For this reason, two phases with an end coil at each side would have different characteristics from another phase. Fig. 13 simply shows a simple flux path at 0°E mover position where the flux path in each core connected in same phase is different due to the end effects. Meanwhile, it can be easily expected that the flux path at 120°E or -60°E mover position would be more symmetric compared to other positions. Therefore, characteristics in linear motor are dependent on the position. Fig. 14 shows the extracted HF inductances according to the mover position. Especially, it can be noted that the linear motor has both characteristics of IPMSM and SPMSM: for example, while the motor has enough saliency in 30°E, L_{dsh} and L_{qsh} are identical in 120°E and -60°E. It means the feasibility of the HF signal injection sensorless methods also depends on the mover position. Even if some researches have been conducted, most of them require the motion of the mover for initial position detection, or unusual design of the mover [25-27]. Therefore, studies on more

practical sensorless drive would be needed.

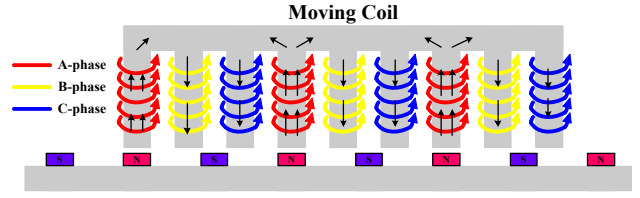


Fig. 12. Structure of the linear motor.

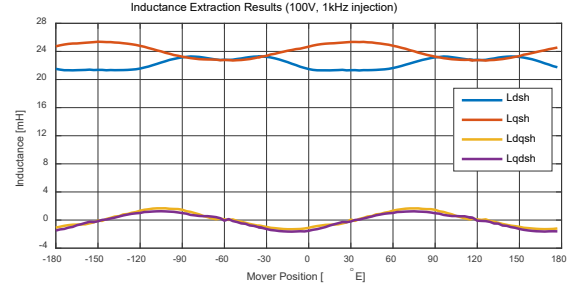


Fig. 13. HF inductances of the linear motor.

It has been well known in industry that the capability of sensorless control based on HF signal injection could be lost in heavy-load condition due to the magnetic saturation of IPMSM. Bianchi *et al.* [23-24] analyzed this issue considering inductance variation according to the load condition and introduced criteria for sensorless control feasibility. This is a challenging issue especially in the traction application; since the motors are designed to be heavily saturated for higher power density, sensorless operation range cannot cover full torque at low speed. The papers clearly mentioned the problems but there is no solution about the problems. Maximizing feasible output torque in low-speed sensorless drive using signal injection with heavily saturated IPMSM is still an open question for the future. The problem might be easily solved by less saturated design of the motor at heavy load condition. But, it cannot be accepted in the traction application, where torque and power density is the premium. However, the performance of sensorless drive can be remarkably improved with the modified design of IPMSM itself, so called sensorless friendly motor. In some application the modified design of IPMSM would be acceptable with its higher performance. With the proper design of IPMSM, the performance of sensorless drive would match to that of the sensor drive with 1024 PPR or higher PPR encoders. In this case the accuracy of the estimation of the rotor position could be better than 1o in electrical angle with 6 pole IPMSM.

As mentioned before, the absolute angle of the rotor was estimated and controlled in sensorless mode. However, there is still necessity of initial rotation for angle identification or extra sensing circuit. Both would be not preferable in the most application. And, the control and motor design for sensorless control of absolute angle of the rotor should be further investigated to remove such disadvantages.

V. CONCLUSION

In this paper, the developments of sensorless control of

interior permanent magnet synchronous machine (IPMSM) for last 10 years have been briefly discussed. Because of intense research and developments there are huge references and industry results in this subject. However, in this paper, only some limited results have been introduced. Most of them in this paper have been developed by a few research groups including the author's one. Authors believe that there are many excellent research results not introduced in this paper. Due to the tremendous effort of peoples in this area, the technology of sensorless drive of IPMSM has been developed rapidly for last 20 years. It has been fully matured and used in various industry fields such as elevators, oil pumps, washing machines, robots, machine tools, etc. The HF signal injection methods have extended the application area of sensorless control remarkably. And, for last 10 years, with better signal processing with higher performance control electronics, and improved understanding of dynamics of IPMSM drive system, and sensorless-friendly design of IPMSM itself, dynamic control range of IPMSM sensorless drive was extended 10 times wider and the accuracy increased 5 times better. For next 5 years, sensorless drive in traction application would be intensively developed with expansion of the market for hybrid and electric vehicle where main tractive effort comes from IPMSM. The sensorless drive system with higher power density IPMSM robust to severe operation conditions and parameter variations should be developed to fulfill the strong demands from automotive industry.

REFERENCES

- [1] N. Matsui, "Sensorless PM brushless DC motor drives," *IEEE Trans. Ind. Electron.*, vol. 43, pp. 300-308, Apr. 1996.
- [2] S. Morimoto, K. Kawamoto, M. Sanada, and Y. Takeda, "Sensorless control strategy for salient-pole PMSM based on extended EMF in rotating reference frame," *IEEE Trans. Ind. Appl.*, vol. 38, pp. 1054-1061, Jul./Aug. 2002.
- [3] Z. Chen, M. Tomita, S. Doki, and S. Okuma, "An extended electromotive force model for sensorless control of interior permanent-magnet synchronous motors," *IEEE Trans. Ind. Electron.*, vol. 50, pp. 288-295, Apr. 2003.
- [4] P. L. Jansen and R. D. Lorenz, "Transducerless position and velocity estimation in induction and salient AC machines," *IEEE Trans. Ind. Appl.*, vol. 31, pp. 240-247, Mar./Apr. 1995.
- [5] M. W. Degner and R. D. Lorenz, "Using multiple saliencies for the estimation of flux, position, and velocity in AC machines," *IEEE Trans. Ind. Appl.*, vol. 34, pp. 1097-1104, Sep./Oct. 1998.
- [6] S. J. Kang, J. M. Kim, and S. K. Sul, "Position sensorless control of synchronous reluctance motor using high frequency current injection," *IEEE Trans. Energy Convers.*, vol. 14, pp. 1271-1275, Dec. 1999.
- [7] M. J. Corley and R. D. Lorenz, "Rotor position and velocity estimation for a salient-pole permanent magnet synchronous machine at standstill and high speeds," *IEEE Trans. Ind. Appl.*, vol. 34, pp. 784-789, Jul./Aug. 1998.
- [8] J. I. Ha and S. K. Sul, "Sensorless field-orientation control of an induction machine by high-frequency signal injection," *IEEE Trans. Ind. Appl.*, vol. 35, pp. 45-51, Jan./Feb. 1999.
- [9] J. H. Jang, S. K. Sul, J. I. Ha, K. Ide, and M. Sawamura, "Sensorless drive of surface-mounted permanent-magnet motor by high-frequency signal injection based on magnetic saliency," *IEEE Trans. Ind. Appl.*, vol. 39, pp. 1031-1039, Jul./Aug. 2003.
- [10] H. Kim, M. C. Härke, and R. D. Lorenz, "Sensorless control of interior permanent-magnet machine drives with zero-phase lag position estimation," *IEEE Trans. Ind. Appl.*, vol. 39, pp. 1726-1733, Nov./Dec. 2003.
- [11] Y. Inoue, K. Yamada, S. Morimoto, and M. Sanada, "Effectiveness of voltage error compensation and parameter identification for model-based sensorless control of IPMSM," *IEEE Trans. Ind. Appl.*, vol. 45, pp. 213-221, Jan./Feb. 2009.
- [12] Y. Inoue, Y. Kawaguchi, S. Morimoto, and M. Sanada, "Performance improvement of sensorless IPMSM drives in a low-speed region using online parameter identification," *IEEE Trans. Ind. Appl.*, vol. 47, pp. 798-804, Mar./Apr. 2011.
- [13] A. Piippo, M. Hinkkanen, and J. Luomi, "Analysis of an adaptive observer for sensorless control of interior permanent magnet synchronous motors," *IEEE Trans. Ind. Electron.*, vol. 55, pp. 570-576, Feb. 2008.
- [14] T. Tuovinen, M. Hinkkanen, L. Harnefors, and J. Luomi, "Comparison of a reduced-order observer and a full-order observer for sensorless synchronous motor drives," *IEEE Trans. Ind. Appl.*, vol. 48, pp. 1959-1967, Nov./Dec. 2012.
- [15] R. W. Hejny and R. D. Lorenz, "Evaluating the practical low-speed limits for back-EMF tracking-based sensorless speed control using drive stiffness as a key metric," *IEEE Trans. Ind. Appl.*, vol. 47, pp. 1337-1343, May/Jun. 2011.
- [16] Y. D. Yoon, S. K. Sul, S. Morimoto, and K. Ide, "High-bandwidth sensorless algorithm for AC machines based on square wave-type voltage injection," *IEEE Trans. Ind. Appl.*, vol. 47, pp. 1361-1370, May/Jun. 2011.
- [17] Y. C. Kwon and S. K. Sul, "Reduction of injection voltage in signal injection sensorless drives using capacitor-integrated inverter," *IEEE Trans. Power Electron.*, vol. 32, no. 8, pp. 6261-6274, Aug. 2017.
- [18] D. Kim, Y. C. Kwon, S. K. Sul, J. H. Kim, and R. S. Yu, "Suppression of injection voltage disturbance for high frequency square wave injection sensorless drive with regulation of induced high frequency current ripple," *IEEE Trans. Ind. Appl.*, vol. 52, no. 1, pp. 302-312, Jan./Feb. 2016.
- [19] S. Kim, J. I. Ha, and S. K. Sul, "PWM switching frequency signal injection sensorless method in IPMSM," *IEEE Trans. Ind. Appl.*, vol. 48, no. 5, pp. 1576-1587, Sep./Oct. 2012.
- [20] Y. C. Kwon, S. K. Sul, N. A. Baloch, S. Murakami, and S. Morimoto, "Design and control of IPMSM sensorless drive for mechanical rotor position estimation capability," *IEEE J. Emerg. Sel. Topics Power Electron.*, vol. 2, no. 2, pp. 152-158, Jun. 2014.
- [21] Y. C. Kwon, S. K. Sul, N. A. Baloch, S. Murakami, and S. Morimoto, "Improved design of IPMSM for sensorless drive with absolute rotor position estimation capability," *IEEE Trans. Ind. Appl.*, vol. 52, no. 2, pp. 1441-1451, Mar./Apr. 2016.
- [22] Y. C. Kwon, S. K. Sul, N. A. Baloch, S. Morimoto, and M. Ohto, "Design, modeling, and control of an IPMSM with an asymmetric rotor and search coils for absolute position sensorless drive," *IEEE Trans. Ind. Appl.*, vol. 52, no. 5, pp. 3839-3850, Sep./Oct. 2016.
- [23] N. Bianchi and S. Bolognani, "Influence of rotor geometry of an IPM motor on sensorless control feasibility," *IEEE Trans. Ind. Appl.*, vol. 43, pp. 87-96, Jan./Feb. 2007.
- [24] N. Bianchi, E. Fornasiero, and S. Bolognani, "Effect of stator and rotor saturation on sensorless rotor position detection," *IEEE Trans. Ind. Appl.*, vol. 49, no. 3, pp. 1333-1342, May/Jun. 2013.
- [25] F. Cupertino, G. Pellegrino, P. Giangrande, and L. Salvatore, "Sensorless position control of permanent-magnet motors with pulsating current injection and compensation of motor end effects," *IEEE Trans. Ind. Appl.*, vol. 47, pp. 1371-1379, May/Jun. 2011.
- [26] T. W. Kim, J. Watanabe, S. Sonoda, and J. Hirai, "New initial pole-position estimation of surface PM-LSM using reference currents," *IEEE Trans. Ind. Appl.*, vol. 41, pp. 817-824, May/Jun. 2005.
- [27] J. K. Seok, T. S. Hwang, and D. H. Kim, "Initial position estimation for closed-loop linear hybrid stepping motor drives using DC excitation," *IEEE Trans. Magn.*, vol. 42, pp. 2071-2076, Aug. 2006.
- [28] K. W. Lee and J. I. Ha, "Evaluation of back-EMF estimators for sensorless control of permanent magnet synchronous motors," *J. Power Electron.*, vol. 12, pp. 604-614, July 2012.
- [29] Y. Park, S. K. Sul, J. K. Ji, and Y. J. Park, "Analysis of estimation errors in rotor position for a sensorless control system using a PMSM," *J. Power Electron.*, vol. 12, pp. 748-757, Sep. 2012.

- [30] Y. Lee, Y. C. Kwon, and S. K. Sul, "Comparison of rotor position estimation performance in fundamental-model-based sensorless control of PMSM," in *Proc. IEEE ECCE 2015*, pp. 5624–5633, Sep. 2015.
- [31] I. Boldea, M. C. Paicu, and G. D. Andreescu, "Active flux concept for motion-sensorless unified AC drives," *IEEE Trans. Power Electron.*, vol. 23, pp. 2612–2618, Sep. 2008.
- [32] A. B. Kulkarni and M. Ehsani, "A novel position sensor elimination technique for the interior permanent-magnet synchronous motor drive," *IEEE Trans. Ind. Appl.*, vol. 28, pp. 144–150, Jan./Feb. 1992.
- [33] S. Ogasawara and H. Akagi, "Implementation and position control performance of a position-sensorless IPM motor drive system based on magnetic saliency," *IEEE Trans. Ind. Appl.*, vol. 34, pp. 806–812, Jul./Aug. 1998.
- [34] V. Petrovic, A. M. Stankovic, and V. Blasko, "Position estimation in salient PM synchronous motors based on PWM excitation transients," *IEEE Trans. Ind. Appl.*, vol. 39, pp. 835–843, May/June 2003.
- [35] M. Schroedel, "Sensorless control of AC machines at low speed and standstill based on the "INFORM" method," in *Conf. Rec. IEEE-IAS Annu. Meeting*, vol. 1, pp. 270–277, Oct. 1996.
- [36] H. Kim and R. D. Lorenz, "Carrier signal injection based sensorless control methods for IPM synchronous machine drives," in *Conf. Rec. IEEE-IAS Annu. Meeting*, vol. 2, pp. 977–984, Oct. 2004.
- [37] S. Ovrebo, "Sensorless control of permanent magnet synchronous machines," Ph.D. dissertation, Dept. of Elect. Power Eng., Norwegian Univ. of Sci. and Tech. (NTNU), Trondheim, 2004.
- [38] D. Raca, P. Garcia, D. Reigosa, F. Briz, and R. Lorenz, "A comparative analysis of pulsating vs. rotating vector carrier signal injection-based sensorless control," in *Proc. IEEE APEC 2008*, pp. 879–885, Feb. 2008.
- [39] H. Kim, K. K. Huh, R. D. Lorenz, and T. M. Jahns, "A novel method for initial rotor position estimation for IPM synchronous machine drives," *IEEE Trans. Ind. Appl.*, vol. 40, pp. 1369–1378, Sep./Oct. 2004.
- [40] C. Caruana, G. M. Asher, and M. Sumner, "Performance of HF signal injection techniques for zero-low-frequency vector control of induction machines under sensorless conditions," *IEEE Trans. Ind. Electron.*, vol. 53, pp. 225–238, Feb. 2006.
- [41] Y. Li, Z. Q. Zhu, D. Howe, C. M. Bingham, and D. A. Stone, "Improved rotor-position estimation by signal injection in brushless AC motors, accounting for cross-coupling magnetic saturation," *IEEE Trans. Ind. Appl.*, vol. 45, pp. 1843–1850, Sep./Oct. 2009.
- [42] D. D. Reigosa, P. Garcia, D. Raca, F. Briz, and R. D. Lorenz, "Measurement and adaptive decoupling of cross-saturation effects and secondary saliencies in sensorless controlled IPM synchronous machines," *IEEE Trans. Ind. Appl.*, vol. 44, pp. 1758–1767, Nov./Dec. 2008.
- [43] Y. Lee and S. K. Sul, "Model-based sensorless control of IPMSM enhancing robustness based on the estimation of speed error," in *Proc. IEEE SLED 2016*, pp. 46–53, Jun. 2016.



Seung-Ki Sul (S'78, M'87, SM'98, F'00)

He received the B.S., M.S., and Ph.D. degrees in electrical engineering from Seoul National University, Seoul, Korea, in 1980, 1983, and 1986, respectively. From 1986 to 1988, he was an Associate Researcher with the Department of Electrical and Computer Engineering, University of Wisconsin, Madison. From 1988 to 1990, he was a Principal Research Engineer with LG Industrial Systems Company, Korea. Since 1991, he has been a member of faculty of School of the Electrical and Computer Engineering, Seoul National University, where he is currently a Professor. He was promoted as a fellow of IEEE with the contribution to PWM technology. Prof. Sul is one of pioneers in the area of carrier based PWM technology applied to the control of the power converters. From 2005 to 2007, he was the Vice Dean of the

Engineering College of Seoul National University. In addition, from 2008 to 2011, he was the President of the Electrical Engineering Science Research Institute funded by the Korean Government. He has published over 145 IEEE journal papers and a total of more than 330 international conference papers in the area of power electronics. He was the program chair of IEEE PESC'06 and general chair of IEEE ECCE-Asia, ICPE, 2011. He holds 14 U.S.A patents, 7 Japanese patents, 11 Korean patents, and granted 43 Ph.Ds under his supervision. The technology regarding sensorless drive of AC machine he worked for last 20 years has been commercialized by many companies such as Yaskawa Electric Co. as general purpose IPM drive, oil pump drive by General Motors Co., and LG Electronics Co. in washing machine. From 2011 to 2014, he had served as Editor-in-Chief of the Journal of Power Electronics, which is a SCIE registered journal, published by the Korean Institute of Power Electronics (KIPE), Seoul, Korea. For year 2015, he was the president of KIPE. He was recipient of 2015 IEEE Transaction 1st and 2nd paper awards on Industrial Application, simultaneously. He was also recipient of 2016 Outstanding Achievement Award of IEEE Industrial Application Society. He was also selected as the recipient of 2017 Newell award sponsored IEEE PELS. His current research interests include power electronic control of electrical machines, electric/hybrid vehicles and ship drives, High Voltage DC transmission based on MMC, and power-converter circuits for renewal energy sources.



Yong-Cheol Kwon was born in Korea in 1986. He received the B.S., M.S., and Ph. D. degrees in electrical engineering from Seoul National University, Seoul, Korea, in 2010, 2012, and 2017, respectively.

He was a Visiting Scholar in Electrical Machines & Drives Group, Electronic and Electrical Engineering department, the University of Sheffield, UK, from 2015 to 2016. He is currently a Senior Researcher in Seoul National University Electric Power Research Institute, Seoul, Korea.

His research interests include power electronics, design and control of electric machines, and sensorless drives.

Dr. Kwon received the 2014 International Power Electronics Conference (IPEC-Hiroshima/ECCE-Asia) First Prize Paper Award and the 2015 IEEE TRANSACTIONS ON INDUSTRY APPLICATIONS Second Prize Paper Award.



Younggi Lee was born in Korea in 1990. He received the B.S. degree in electrical engineering in 2013 from Seoul National University, Seoul, Korea, where he is currently working toward the Ph.D. degree. His current research interests include power electronics, control of electric machines, electric/hybrid vehicles, and sensorless drive.